JOURNAL OF VIROLOGY, Feb. 2002, p. 1856–1865 Vol. 76, No. 4
0022-538X/02/$04.00+0 DOI: 10.1128/JVI.76.4.1856–1865.2002

Internalization of Echovirus 1 in Caveolae

Varpu Marjomäki,[1]* Vilja Pietiäinen,[2] Heli Matilainen,[1] Paula Upla,[1] Johanna Ivaska,[3] Liisa Nissinen,[3] Hilkka Reunanen,[1] Pasi Huttunen,[2,3] Timo Hyypiä,[2] and Jyrki Heino[1,3]

Department of Biological and Environmental Science, University of Jyväskylä, FIN-40351 Jyväskylä,[1] Haartman Institute, Department of Virology, University of Helsinki, FIN-00014 Helsinki,[2] and MediCity Research Laboratory and Department of Medical Biochemistry, University of Turku, FIN-20520 Turku,[3] Finland

Received 2 July 2001/Accepted 6 November 2001

Echovirus 1 **(EV1) is a human pathogen which belongs to the *Picornaviridae* family of RNA viruses. We have analyzed the early events of infection after EV1 binding to its receptor α2β1 integrin and elucidated the route by which EV1 gains access to the host cell. EV1 binding onto the cell surface and subsequent entry resulted in conformational changes of the viral capsid as demonstrated by sucrose gradient sedimentation analysis. After 15 min to 2 h postinfection (p.i.) EV1 capsid proteins were seen in vesicular structures that were negative for markers of the clathrin-dependent endocytic pathway. In contrast, immunofluorescence confocal microscopy showed that EV1, α2β1 integrin, and caveolin-1 were internalized together in vesicular structures to the perinuclear area. Electron microscopy showed the presence of EV1 particles inside caveolae. Furthermore, infective EV1 could be isolated with anti-caveolin-1 beads 15 min p.i., confirming a close association with caveolin-1. Finally, the expression of dominant negative caveolin in cells markedly inhibited EV1 infection, indicating the importance of caveolae for the viral replication cycle of EV1.**

Efficient entry of viruses into host cells and release of the viral genome are essential steps in the initiation of the infection cycle. Viruses have adapted to utilize various cell surface molecules as their receptors which often seem to direct the virus to use the clathrin-dependent pathway (23). However, other entry mechanisms may also mediate the endocytosis of viruses (3). The present understanding about non-clathrin-coated endocytosis of viruses is mainly based on the entry mechanism of simian virus 40 (SV40) through caveolae (24, 28, 29). Caveolae are caveolin-1-containing specific lipid invaginations in the plasma membrane, involved in cholesterol trafficking and potocytosis of small molecules (27). They also contain molecules that play pivotal roles in intracellular signal transduction (20).

An important question is whether the cell surface receptor interacting with the virus can regulate the entry process and guide the virus to a specific endocytosis route. One group of cell surface proteins, the integrins, is recognized by many viruses and can be used to study the role of virus receptors in the internalization process in general. The integrins are a large family of heterodimeric cell surface receptors mediating cell-extracellular matrix and cell-cell adhesion (14). Their natural ligands include extracellular matrix proteins, such as collagens, fibronectin, laminins, and tenascin, and also members of the immunoglobulin superfamily. Although many integrins recognize a short motif of three amino acids, arginine-glycine-aspartic acid (RGD), in their ligands (30), the function of most members of the family is RGD independent.

Picornaviruses are small, nonenveloped RNA viruses which include several important human and animal pathogens. Echoviruses belong to the enterovirus genus of the *Picornaviridae* family and cause meningoencephalitis, carditis, and rashes as well as mild respiratory and enteric diseases (10). Echovirus 1 (EV1) binds to α2β1 integrin, a collagen receptor (6), on the cell surface. Although the receptors of several members of the family have already been identified (9, 32, 33) the internalization process of picornaviruses has remained largely unclear. We demonstrate here that, unlike many other viruses, EV1 is not found in compartments associated with the clathrin-dependent internalization route. Instead, caveolae are involved in EV1 internalization. During virus entry, caveolin-1 and α2β1 integrin colocalize with EV1 viral capsid proteins and migrate into the perinuclear area in the cell. Expression of dominant negative caveolin in cells inhibits EV1 infection, confirming the essential role of caveolae for the EV1 entry. Internalization of EV1 represents an entry mechanism that has not been previously described for any other picornavirus, demonstrating the importance of the caveola route in the internalization of human viral pathogens.

MATERIALS AND METHODS

Cells, antibodies, and reagents. SAOS cells (American Type Culture Collection [ATCC]), which do not normally express the α2 integrin subunit, were stably transfected with an expression construct encoding the α2 integrin (SAOS-α2β1 cells) (15). The α2/α1 integrin mutant contained the intracellular tail of the α1 integrin subunit (SAOS-α2/α1β1 cells) (15). SAOS-pAW cells, which contain an empty expression vector, were used as a control in the experiments. The following antibodies were used: monoclonal antibodies (MAbs) against integrin α2 subunit (12F1, BD Pharmingen; MAB1950, Chemicon); rabbit antiserum (Transduction Laboratories) as well as MAbs (Transduction Laboratories, Zymed) against caveolin-1; rabbit antiserum against the cation-independent mannose 6-phosphate receptor (CI-MPR) (21); rabbit antisera (GB2) against *trans*-Golgi network protein 46 (TGN-46) (4), p23 (34), and early endosome antigen 1 (EEA1) (22); MAb 1D3 to detect protein disulfide isomerase (PDI) (13), rabbit antibody (AB730; Chemicon), as well as MAb (BM-63, Sigma) against human β2 microglobulin; MAb against class I HLA (W6/32) (5); MAb against hemagglutinin (HA) tag (Santa Cruz); rabbit antibody against human parechovirus (HPEV1) capsid proteins (16); and MAb against myc peptide (ATCC) to reveal a transferrin receptor (a kind gift from H. Garoff) (39) chimera with myc tag. Rabbit antiserum against purified EV1 was produced as follows.

* Corresponding author. Mailing address: Department of Biological and Environmental Science, University of Jyväskylä, FIN-40351 Jyväskylä, Finland. Phone: 358-14-2602273. Fax: 358-14-2602221. E-mail: vmarjoma@cc.jyu.fi.

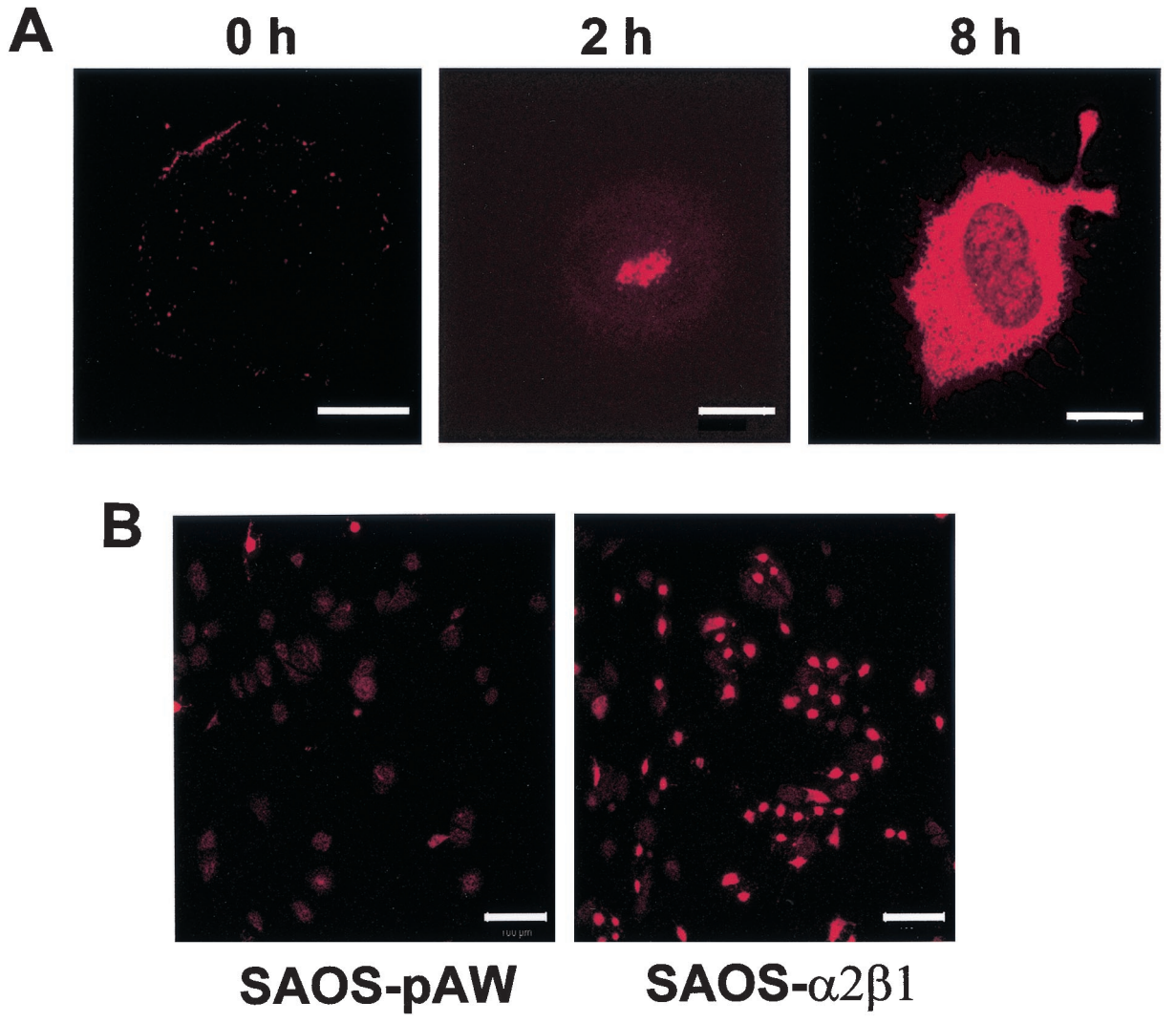

FIG. 1. (A) Immunofluorescent labeling of EV1 using anti-EV1 rabbit hyperimmune serum in SAOS-α2β1 cells after viral attachment (0 h), 2 h p.i., or 8 h p.i. (Bars = 10 μm). (B) Low-magnification picture of anti-EV1 labeling in α2β1-negative vector control SAOS-pAW cells and in SAOS-α2β1 cells 10 h p.i. (Bars = 100 μm).

Purified EV1 was used for immunization of rabbits by primary subcutaneous injection containing 15 μg of the virus in Freund's complete adjuvant, followed by booster doses of 10 μg in incomplete adjuvant 4 and 8 weeks later. The serum was collected 3 weeks after the last injection. When the antiserum was incubated with overlapping peptides covering the capsid proteins of EV1, most reactivity was observed with VP1, and some reactivity was also observed with the VP2 and VP3 peptides (P. Huttunen and T. Hyypiä, unpublished). Anti-EV1 antiserum had no cross-reactivity with the SAOS cells (Fig. 1B and 2A). Methyl β-cyclodextrin was obtained from Sigma.

Virus preparations. EV1 (Farouk strain) was obtained from the ATCC, and the virus was propagated in GMK or LLC cells. To obtain radioactively labeled EV1, infected GMK cells were incubated with [^{35}S]methionine (50 μCi/ml; Pharmacia Biotech) in MEM without L-methionine (GibcoBRL, Life Technologies). The virus was purified in sucrose gradients as described previously (1). The infectivity of purified virus was determined by plaque titration. To infect cells, purified EV1 was used at a multiplicity of infection of 20, if not otherwise stated. Purified HPEV1 was also used in some experiments (16).

Infectivity titration. Confluent SAOS-α2β1 and SAOS-α2/α1β1 cells, infected with EV1, were harvested after different time periods. Three freeze-thaw cycles were performed to disrupt the cells, and the supernatant containing the virus was collected after centrifugation. The amount of intracellular virus synthesized in the SAOS cell lines was determined at dilutions of 10^{-1} to 10^{-12} in GMK cells. After incubation for 7 days at 37°C, the cells were stained with crystal violet and the amount of infectious virus was expressed as end point titers.

Binding assay for EV1. SAOS-pAW and SAOS-α2β1 cells (200,000 cells/assay) were suspended into 30 μl of phosphate-buffered saline (PBS) containing 2 mM $MgCl_2$ (PBS-$MgCl_2$). [^{35}S]methionine-labeled EV1 (75,000 cpm) was added on the cells and incubated for 1 h on ice. The cells were washed twice with PBS-$MgCl_2$, and the pellet was suspended in PBS and analyzed for radioactivity in a scintillation counter (1450 Microbeta; Wallac).

Analysis of conformational changes of EV1 by sucrose gradient sedimentation. Confluent SAOS-α2β1 cells were detached in 0.02% Versene in PBS, pelleted, and washed twice with PBS. For the attachment of the virus, the cells were suspended in PBS-$MgCl_2$, 150,000 cpm of [^{35}S]methionine-labeled EV1 was added, and cells were incubated for 1 h on ice. The cells were then washed twice with PBS-$MgCl_2$ to remove any unbound virus and incubated at 37°C from 0 to 2 h in Dulbecco's MEM, containing 1% fetal calf serum. After cell lysis with 1% Triton X-100 (10 min on ice) and low-speed centrifugation, the supernatant was layered on a 5 to 20% (wt/vol) sucrose gradient and centrifuged for 2 h at 4°C and 150,000 × *g* in a Beckman SW41Ti rotor. Fractions (500 μl) were collected and analyzed for radioactivity in a scintillation counter. Samples containing only radiolabeled EV1 were used as control.

Immunoperoxidase staining for EV1. For immunoperoxidase staining experiments, the confluent SAOS-α2β1 cell monolayers in 24-well plates were first

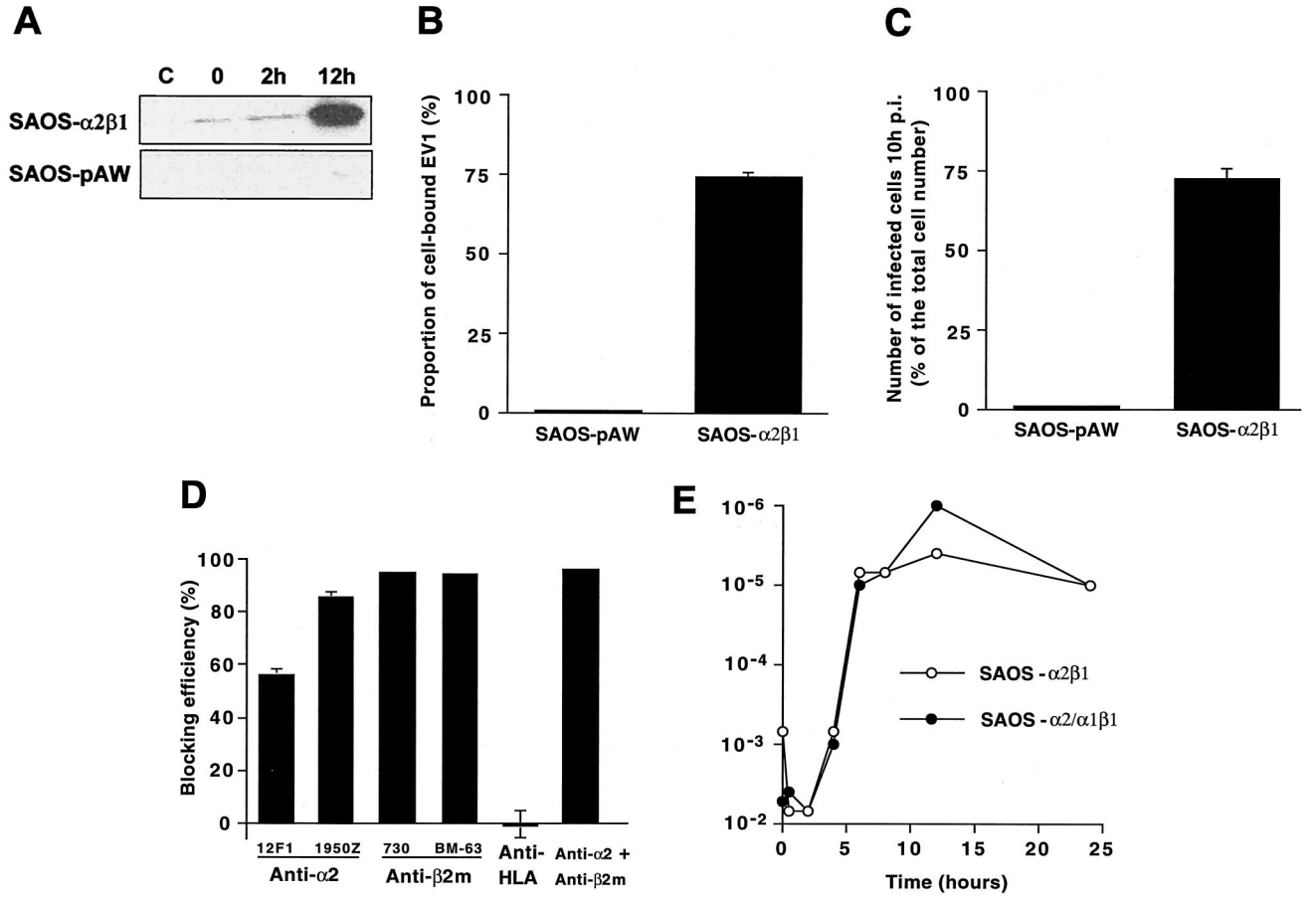

FIG. 2. (A) Western blot of SAOS-pAW and SAOS-α2β1 cell homogenates without EV1 infection (C) or 0, 2, or 12 h p.i. (B) Binding of radioactively labeled EV1 onto SAOS-pAW and SAOS-α2β1 cells. (C) The proportional number of infected cells in SAOS-pAW and SAOS-α2β1 cells 10 h p.i. calculated after immunoperoxidase labeling. (D) The blocking effect of various antibodies on EV1 infection 10 h p.i. calculated after immunoperoxidase labeling (antibodies used in combination are 1950Z for anti-α2 and AB730 for anti-β2m). (E) Production of infectious EV1 in SAOS-α2β1 and SAOS-α2/α1β1 cells. The amount of intracellular virus in SAOS cells was determined in GMK cells as end point titers.

incubated with a 1:100 dilution of different antibodies: anti-α2 integrin (12F1 and MAB1950Z), anti-β2 microglobulin (AB730 and BM-63/M-7398), and anti-HLA-I (W6/32) or their combinations (15 min at room temperature). Purified EV1 was then added, and after 10 h at 37°C, methanol-fixed cells were incubated with anti-EV1 rabbit antiserum (1:100) and then with peroxidase-labeled goat anti-rabbit antibody (Dako). The cells were stained with chromogen solution containing H_2O_2 in a 1:1,000 dilution, and the reaction was stopped by washing cells twice with PBS (48). The proportion of infected cells was counted under a light microscope.

Immunofluorescence and confocal microscopy. Subconfluent SAOS-α2β1 cultures were infected by EV1 for various time periods and then fixed with cold methanol at −20°C for 6 min. Highly cross-absorbed goat secondary antibodies against rabbit (Alexa red, 546 nm; Molecular Probes, Inc.) and mouse (Alexa green, 488 nm; Molecular Probes, Inc.) antibodies were used in the labelings. The dilutions of the secondary antibodies used in the experiments gave negligible background. Nonspecific reactions between primary and secondary antibodies were not observed. The cells were mounted in mowiol and examined with an Axiovert 100 M SP epifluorescence microscope (Carl Zeiss) and a confocal microscope (Zeiss LSM510). For double-labeling experiments, multitracking for 488- and 546-nm laser lines was used in order to avoid false colocalization. In order to quantitate EV1 from the scanned cells, four slices from the center (2 μm in total) were selected and projected together. From this projection, a histogram of intensity values was prepared with LSM510 program. A threshold value of 100 was selected for all the samples, and all intensity values from 100 to 250 were plotted. Frequency values were multiplied by the respective intensities, and the results were summed up for each sample. Statistical comparisons were performed using nonparametric Kruskal-Wallis one-way analysis of variance (Mann-Whitney U test). The double labeling images of EV1, caveolin-1, and α2β1 integrin (see Fig. 4 and 7) are representative of at least 100 similar images.

Immunoisolation. Subconfluent monolayers were infected with EV1 for different periods of time as described above. After infection, the cells were scraped from the dishes into PBS and pelleted (150 × *g*, 5 min, 4°C). The pellet was washed with homogenization buffer (3 mM imidazole, 0.25 M sucrose, 1 mM EDTA [pH 7]) and pelleted again. Homogenization was carried out in homogenization buffer by passing the pellet extensively through a 23-gauge needle. The homogenate was pelleted at 600 × *g* for 10 min at 4°C, and 100 μg of the postnuclear supernatant was then subjected to immunoisolation. M-450 Dynal beads (Dynal AS), coated with sheep anti-mouse immunoglobulin G (IgG), were pretreated the previous day by washing two times with PBS. Beads (2×10^7) were then coated overnight with 3.75 μg of mouse anti-caveolin-1 (clone 2234, Transduction Laboratories) or 3.75 μg of nonspecific mouse IgG (Sigma) together with 1% bovine serum albumin (BSA). The coating was carried out overnight using end-over-end mixing, and the beads were then washed twice with PBS. The beads were incubated with the homogenates for 1 h by rotating end over end at 4°C. The UB fraction was stored for further analysis, and the beads were washed twice with PBS. The homogenate, a sample from the UB fraction, and the beads were diluted in Laemmli sample buffer and subjected to sodium dodecyl sulfate (SDS)-polyacrylamide gel electrophoresis and immunoblotting. EV1 and caveolin-1 were visualized by rabbit anti-caveolin-1 or anti-EV1 antiserum, followed by anti-rabbit horseradish peroxidase conjugate (Bio-Rad) and chemiluminescent Super Signal substrate (Pierce).

Plaque titration for EV1 isolated from infected cells using anti-caveolin-1 beads. In order to measure the infectivity of the virus particles inside the caveola structures the immunoisolated material was treated with 0.5% SDS for 15 min on

ice to release the virus from caveola structures. After centrifugation (1 min, 4°C, 16,000 × *g*) the samples were diluted from 10^{-2} to 10^{-5} to 0.6% fetal bovine serum in Hanks' solution. The dilutions were incubated on confluent GMK cells at 37°C for 30 min, and the cells were then overlayered with carboxymethylcellulose. The cells were incubated for 2 days prior to staining with crystal violet and counting the average amount of the plaques in four parallel wells. The experiment was performed four times.

Transfection experiments. Subconfluent SAOS-α2β1 cells were transfected with HA-tagged wild-type caveolin-3 and dominant negative mutant caveolin-3 (Cav^{DGV}) (36). Transfection was carried out using Fugene 6 reagent (Boehringer Mannheim) according to the manufacturer's instructions. After a 48-h incubation period the cells were infected with EV1. Ten hours postinfection (p.i.), the cells were methanol-fixed and incubated with antibodies against HA tag and EV1, followed by secondary antibodies. The number of transfected and infected cells was calculated using confocal microscopy. As a control experiment, transfection was also carried out in A549 cells as described above. After 48 h of incubation the cells were infected with HPEV1 (multiplicity of infection, 10) for 6 h. The cells were then fixed in methanol and labeled with antibodies against HPEV1 capsid proteins (rabbit polyclonal) (16) and mouse antibody against HA tag.

Electron microscopy. Monolayers of SAOS-α2β1 cells were fixed in 2.5% glutaraldehyde in 0.1 M phosphate buffer (pH 7.4) for 1 h, and then postfixed in 1% osmium tetroxide for 1 h in the same buffer, dehydrated in ethanol, stained with uranyl acetate, and embedded in LX-112. When internalization of EV1 via caveolae was studied, EV1 was first allowed to bind to cells for 1 h on ice and then washed three times with PBS containing bovine serum albumin (0.5 mg/ml). Cells were then incubated with EV1 antibodies for 1 h on ice, washed and treated with protein A-gold (5-nm-diameter particles; G. Posthuma and J. Slot, Utrecht, The Netherlands), also for 1 h on ice, and washed as described above. Protein A-gold dilutions that gave no nonspecific labeling were chosen. Cells were then either fixed immediately or allowed to internalize EV1 at 37°C in complete culture medium. Further preparation for electron microscopy was performed as described above. SAOS-pAW control cells treated with EV1 were negative for protein A-gold label, showing that immunolabeling was specific (data not shown). Samples for cryo-ultramicrotomy were fixed and processed as described previously (21).

RESULTS

Integrin α2β1 and β2 microglobulin are required for efficient EV1 infection in SAOS-α2β1 cells. We have previously generated human osteosarcoma SAOS cell clones transfected with α2 integrin cDNA (SAOS-α2β1 cells) (15). One hour after the attachment of purified EV1 onto the cells on ice (indicated as 0 h p.i.), speckled staining was observed on SAOS-α2β1 cells with anti-EV1 rabbit antiserum (Fig. 1A). Interestingly, EV1 was observed in an intracellular location 2 h p.i. (Fig. 1A), clearly before the actual virus production took place (5 to 10 h p.i.) (Fig. 2E). Anti-EV1 staining of control SAOS-pAW cells, transfected with an empty vector, showed very low signal, confirming the previous observations that α2β1 integrin is needed for EV1 infection (Fig. 1B). Immunoblotting of SAOS-pAW and SAOS-α2β1 cell homogenates showed that only in SAOS-α2β1 cells was there a clear increase in the amount of EV1 capsid proteins 12 h p.i. (Fig. 2A). In addition, the blot confirmed that the antiserum does not bind nonspecifically to cellular proteins. In accordance with these results, a binding assay with radioactively labeled EV1 showed that only 0.5% of virus was bound onto SAOS-pAW cells, compared to over 70% binding onto SAOS-α2β1 cells (Fig. 2B).

The possible role of other putative receptors in the initiation of infection was studied by inhibiting the infection by specific antibodies. HLA-1 may participate in the entry of SV40 (38), and β2 microglobulin may be involved in the entry process of certain picornaviruses (42). The cells were preincubated with antibodies against the cell surface molecules and infected with the virus. Ten hours p.i., the number of infected cells was determined by EV1 antiserum using immunoperoxidase staining. In the experiments only a small proportion of control SAOS-pAW cells were positive for viral antigens (Fig. 2C). When SAOS-α2β1 cells were preincubated with antibodies against α2β1 integrin, 12F1 reduced the infectivity by 56% ± 2%, whereas MAB1950 was more efficient and reduced the infectivity by 86% ± 1% (Fig. 2D). Two antibodies against β2 microglobulin, AB730 and BM-63, also reduced the infection efficiently (blocking effect was 95% ± 0.2% and 94% ± 0.3% for AB730 and BM-63, respectively) (Fig. 2D). When cells were pretreated with a combination of anti-α2 integrin and anti-β2 microglobulin antibodies, the infection decreased by 96% ± 0.2%. On the other hand, an antibody against HLA-1, which is expressed in association with β2 microglobulin on the cell surface, did not have any apparent effect on infection (Fig. 2D). These results support the previous finding that antibodies against β2 microglobulin have an inhibitory effect on EV1 infection (42). Whether this protein is directly involved in EV1 entry needs further investigation.

To study the role of the intracellular domain of α2 integrin subunit in EV1 infection, the SAOS cells were transfected with a cDNA construct coding for a chimeric α subunit in which the intracellular part of the α2 subunit was replaced by the corresponding sequence of the α1 subunit. In accordance with previous studies (18), the mutation of the cytoplasmic domain of α2 integrin had little if any effect on the replication of EV1 in cell culture (Fig. 2E).

The structural changes in the virus particle during the early events of the infection were also analyzed. Radiolabeled EV1 particles were allowed to attach to cell surface for 1 h on ice, and subsequently, the temperature was shifted to 37°C for 0.5 to 2 h. The cells were collected, and the sedimentation of cell-associated virus was analyzed in sucrose gradients (Fig. 3). It is known that native poliovirus 1 sediments at 160S, and particles that have lost the VP4 polypeptides sediment at 135S while 80S particles represent empty capsids lacking also the RNA genome. Sucrose gradient analysis showed that prior to binding to the cells, the virus sedimented exclusively as the 160S form. After 1 h of incubation on ice, EV1 associated with SAOS-α2β1 cells sedimented as 160S and approximately 135S particles, where the latter ones predominated (40% ± 10% in the 160S form and 55% ± 5% in the so-called 135S form, expressed as mean values of three independent measurements) (Fig. 3A). Thirty minutes to 2 h p.i. incubation at 37°C resulted in the appearance of 80S empty capsids (30 min p.i., 25% ± 5%, 2 h p.i., 35% ± 5%) (Fig. 3B).

Integrin α2β1 is internalized in association with EV1. EV1-infected SAOS-α2β1 cells were double-labeled with antibodies against EV1 and α2 integrin subunit (Fig. 4A). Colocalization of integrin α2 subunit with β1 subunit was confirmed in separate experiments, which indicated that α2 is not expressed alone but as the α2β1 heterodimer as expected (not shown). Attachment of EV1 onto the plasma membrane did not cause any apparent alteration in the distribution of the integrin, and colocalization of EV1 and α2β1 integrin was most obvious on the cell boundaries (Fig. 4A). However, perinuclear localization of EV1 in some SAOS-α2β1 cells (12%) was already seen after 5 min of incubation at +37°C. Interestingly, EV1 colocalized in the perinuclear accumulations with α2β1 integrin. Thirty minutes p.i., 30% of the cells showed perinuclear accu-

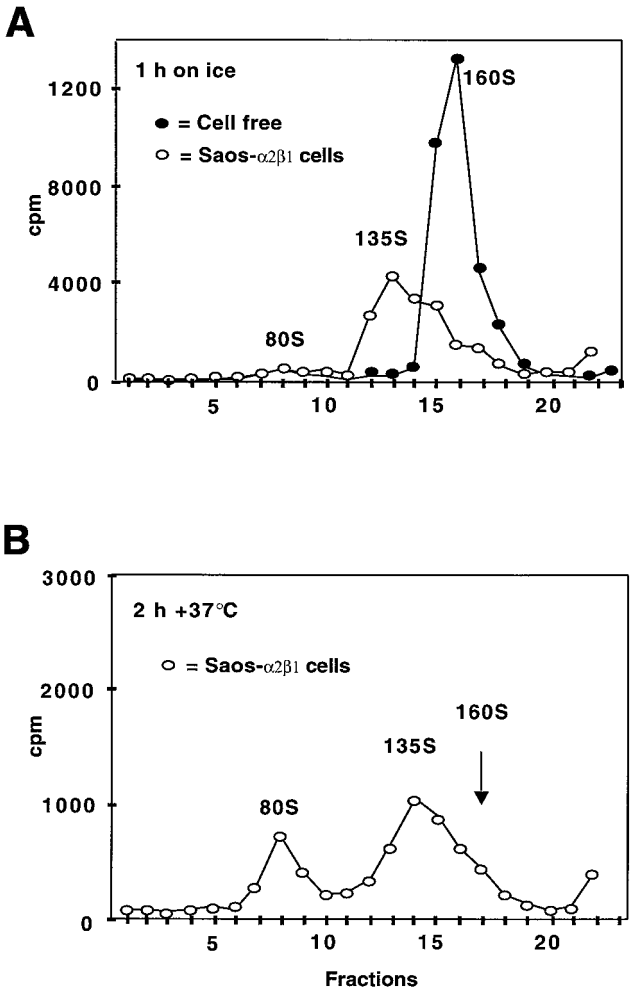

FIG. 3. (A and B) Sucrose gradient sedimentation analysis of conformational changes in EV1 capsid structure during attachment and entry to the cells. After incubation of the SAOS-α2β1 cells with EV1 for 1 h on ice (A), they were transferred to 37°C for 2 h (B).

mulation of α2β1 integrin and EV1. This redistribution increased in a linear manner during the first hours of infection, and at 2 h p.i., already 70% of the cells showed perinuclear colocalization of EV1 and α2β1 integrin (Fig. 4A). Although α2β1 integrin and β2 microglobulin exhibited some colocalization on the cell surface after EV1 attachment (not shown), double-labeling experiments 2 h p.i. indicated that there was no significant colocalization of β2 microglobulin with α2 integrin subunit in the perinuclear region (Fig. 4B).

Internalized EV1 and α2β1 integrin do not colocalize with markers of the clathrin-dependent endocytosis route. Many viruses use the clathrin-dependent endocytic route when entering the cell. We used EEA1 as a marker for early endosomes (22) and transferrin receptor (TF) as a marker for early sorting and recycling endosomes (11). In order to visualize the TF, a myc-tagged transferrin receptor (TF-myc) construct was expressed in the cells by using a Semliki Forest virus expression system prior to EV1 infection.

Our recent studies on another picornavirus, HPEV1, showed that this virus uses the clathrin-dependent pathway and thus accumulates in EEA1-positive early endosomes and CI-MPR-positive late endosomes after 5 and 30 min, respectively (16). However, we found no colocalization of EV1 with EEA1 or TF-myc, suggesting that EV1 did not enter the cells through early endosomes (Fig. 5). Similarly, staining with TGN-46 antibody (labels the *trans*-Golgi network [4]), p23 antibody (a marker for the *cis*-Golgi network [34]; not shown) and CI-MPR (found primarily in the late endosomes) revealed no detectable colocalization with α2β1 integrin or EV1 (Fig. 5).

Concomitant internalization of EV1 and α2β1 integrin with caveolin-1. Electron micrographs indicated that the surface of SAOS-α2β1 cells is rich in caveolae (Fig. 6A). Incubation of infected cells for 30 min at 37°C caused the appearance of EV1 in vesicular structures with characteristics of caveolae (spherical vesicles, approximately 60 to 90 nm in diameter and without a visible coat) (Fig. 6B and C). Caveola-like vesicles were observed in the peripheral cytoplasm, close to the plasma membrane, but in some cells also near the nucleus in large accumulations (Fig. 6D). Colocalization of caveolin-1 and EV1 was shown by double immunolabeling of cryosections (Fig. 6E and F), further confirming that the EV1-containing vesicles represent caveolae. After 2 h of incubation at 37°C, some of the internalized structures seemed to be surrounded by a limiting membrane (Fig. 6D). It is possible that the membrane-containing viral capsid proteins may have been taken up by autophagy or that capsid proteins may have entered a preexisting membranous organelle, e.g., smooth-surface endoplasmic reticulum (ER).

Confocal microscopy showed scattered, small-vesicular distribution of caveolin-1 in uninfected SAOS-α2β1 cells (not shown) and in infected SAOS-α2β1 cells immediately after EV1 attachment (Fig. 7A). However, between 30 min and 2 h p.i., caveolin-1 showed considerable perinuclear staining (Fig. 7B) and colocalization with EV1 (Fig. 7C) and α2β1 integrin (Fig. 7D) in characteristic perinuclear vesicular accumulations. After 2 h p.i., caveolin-1 and α2 integrin were colocalized in 74% of the cells, and caveolin-1 colocalized with EV1 in intracellular structures in 73% of the cells, suggesting that the viral capsid polypeptides, the integrin, and caveolin-1 were codistributed to perinuclear structures during the infection.

Kartenbeck et al. (17) and Pelkmans et al. (29) have shown that 3 to 5 h p.i., SV40 enters the ER. In EV1 infection, double-labeling with PDI, a marker for ER, showed no colocalization (data not shown), indicating that the EV1–integrin–caveolin-1 complex did not enter ER during the first 2 h p.i. However, it is possible that EV1 capsid proteins could enter the smooth-surfaced part of the ER which does not accumulate PDI.

EV1 capsid proteins can be isolated in association with caveolin-1. In order to confirm the association of EV1 with caveolae we used a protocol developed by Oh and Schnitzer (26) and modified by us to immunoisolate caveola structures. In the isolation protocol we used an antibody that recognizes caveolin-1 in intact caveola structures but not caveolin-1 that is outside these structures (26). After EV1 had attached to the receptor, a significant fraction of viral proteins could already be isolated with anti-caveolin-1 beads, suggesting that EV1 may bind directly to caveola-like membrane domains (Fig. 8). Incubation of the cells for 15 min at 37°C increased the amount of EV1 in caveolae. In contrast, EV1 was not enriched when

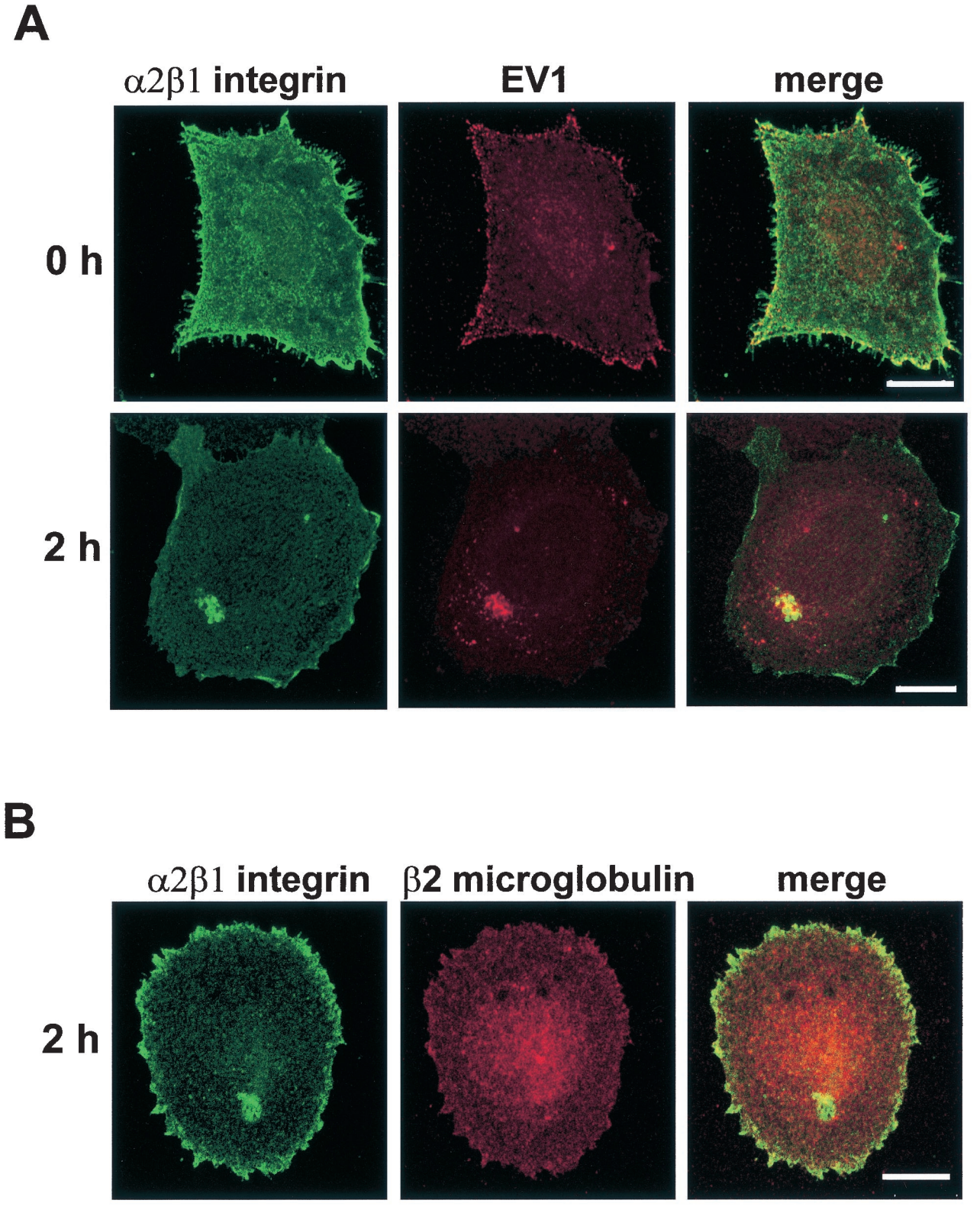

FIG. 4. (A) Colocalization of α2β1 integrin (green) with EV1 (red) in SAOS-α2β1 cells after viral attachment on ice (0 h) or after 2 h of infection at 37°C. (B) Double-labeling with anti-β2 microglobulin and anti-α2 integrin antibodies 2 h p.i. Colocalization is visualized as the yellow color in merge images. Bar = 10 μm.

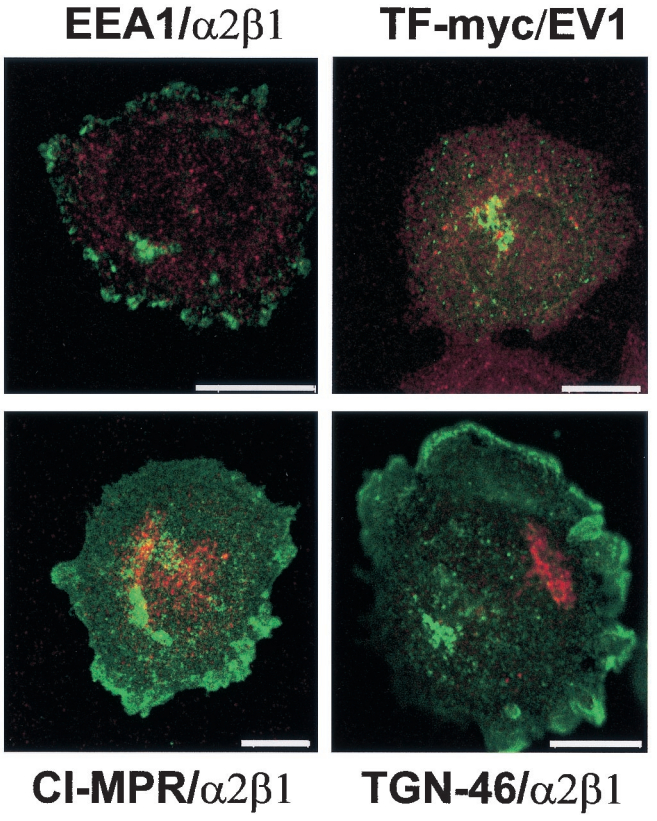

FIG. 5. Double-labeling of EV1-infected SAOS-α2β1 cells with EV1 antiserum or anti-α2β1 integrin antibody together with markers connected to the clathrin-dependent endocytic route. EEA1/α2β1, α2β1 integrin (green) with the early endosomal marker EEA1 (red); TF-myc/EV1, EV1 capsid proteins (red) with the myc-tagged transferrin receptor, a marker for the early endosomes (green); CI-MPR/α2β1, α2β1 integrin (green) with late endosomal marker (red); TGN-46/α2β1, α2β1 integrin (green) with Golgi marker TGN-46 (red). Bar = 10 μm.

isolated with control beads coated with nonspecific mouse IgG from the same homogenate samples, confirming that the protocol was specific for caveolae (Fig. 8). In addition, we could isolate a larger amount of α2β1 integrin with anti-caveolin-1 antibodies 15 min p.i. than after virus binding on cells (0 h p.i.), suggesting that also α2β1 integrin is recruited to caveolae shortly after virus binding (data not shown).

We further tested whether the immunoisolated caveola structures contain virus particles that are still infectious. We treated the immunoisolated structures with 0.5% SDS for 15 min in order to release the virus particles. The plaque titration

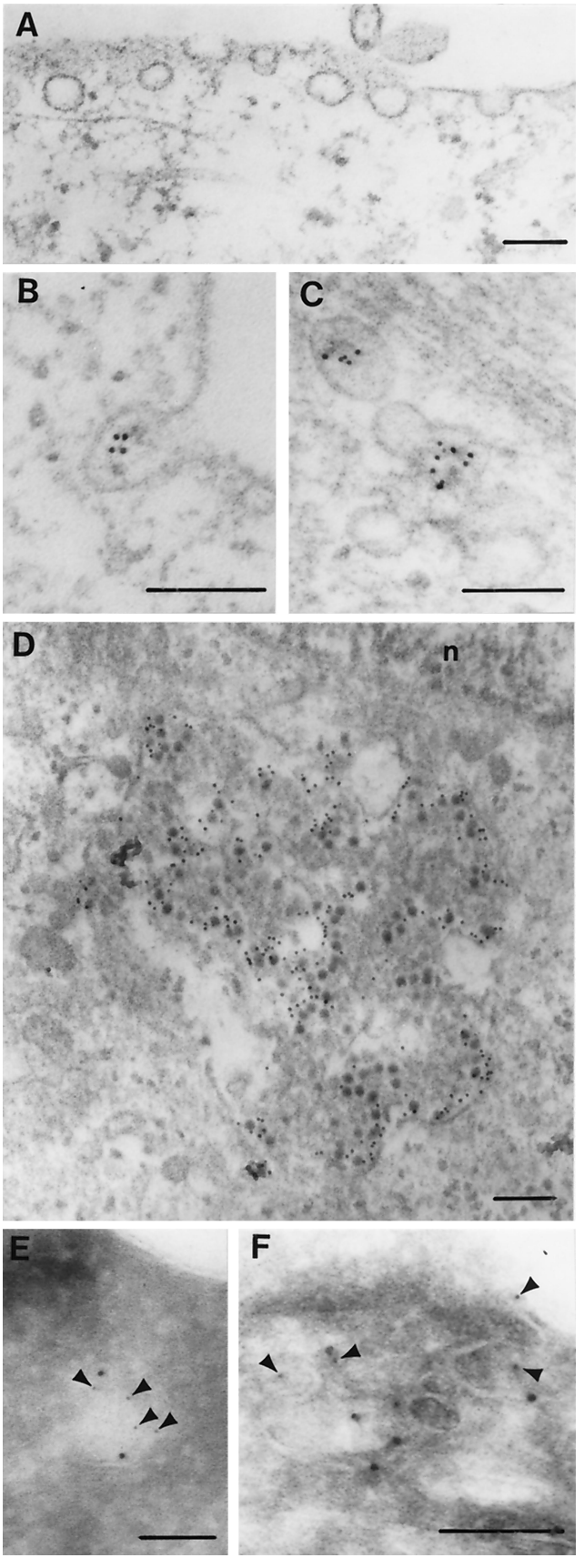

FIG. 6. Electron micrographs of caveolae in SAOS-α2β1 cells. (A) Section of an uninfected cell showing several caveolae. (B to D) Immunolocalization of EV1 (5 nm proteinA-gold) in a caveola-like membrane invagination (B), in a cluster of caveolae deeper in the cytoplasm 30 min p.i. (C), and in a large accumulation close to the nucleus (n) 2 h p.i. (D). (E and F) Double cryo-immunolabeling of caveolin-1 (10-nm-diameter protein A-gold particles) and EV1 (5-nm-diameter protein A-gold particles) in a caveola-like structure close to the plasma membrane (5-nm-diameter protein A-gold particles are indicated by arrowheads). Bars = 100 nm.

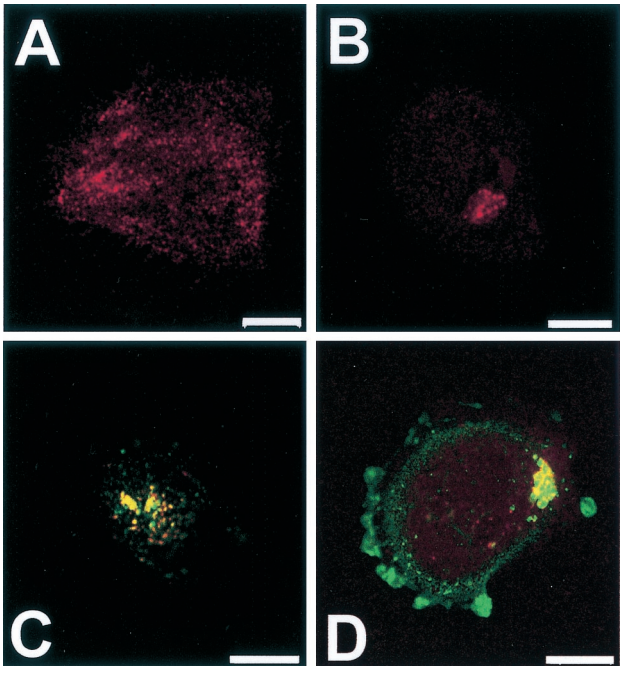

FIG. 7. Labeling of caveolin-1 in SAOS-α2β1 cells after viral attachment (A) and 2 h p.i. (B). (C) Double-labeling of caveolin-1 (green) with EV1 (red) after 2 h p.i. (D) Caveolin-1 (red) with α2β1 integrin (green) after 2 h p.i. Colocalization is visualized as a yellow color in merged images (C and D). Bar = 10 μm.

showed that immunoisolated caveola structures contained infective virus. The samples immunoisolated with anti-caveolin-1 beads produced 22 ± 6 plaques (10^{-4} dilution), while control beads gave only 0.3 ± 0.3 plaques (mean value of four parallel measurements). In the same experiment, SDS-treated postnuclear supernatant gave 220 ± 10 plaques.

Dominant negative caveolin inhibits EV1 infection. To verify the role of caveolae in EV1 entry, an expression construct coding for dominant negative caveolin (36) was transfected into SAOS-α2β1 cells, and the proportion of EV1-infected cells among the transfected cells was calculated (Table 1). Expression of wild-type caveolin had no effect on EV1 infection, whereas dominant negative caveolin (Cav^{DGV}) caused a 66% inhibition of infection (mean value for the three separate experiments) (Table 1), suggesting that intact caveolae are essential for the initiation of an efficient EV1 replication cycle.

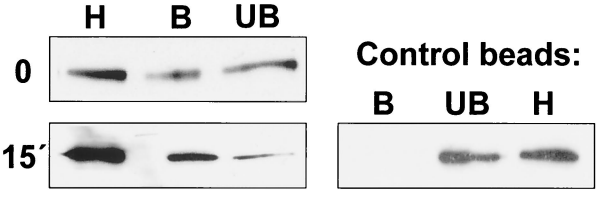

FIG. 8. Immunoisolation of caveola structures with anti-caveolin-1 Dynal beads. Immunoisolation was performed in SAOS-α2β1 cells after viral attachment (0) or 15 min p.i. The Western blot has been stained with anti-EV1 antiserum. Dynal beads coated with nonspecific mouse IgG were used as control. Abbreviations: H, homogenate; B, bound fraction. UB, unbound fraction.

TABLE 1. Proportion of EV1-infected cells among transfected cells with wild-type caveolin-3 (Cav) or dominant negative caveolin (Cav^{DGV})[a]

Expt no.	Mean proportion of cells infected ± SE (*n*)		
	Not transfected	Cav	Cav^{DGV}[b]
I	0.32 ± 0.02 (208)	0.32 ± 0.01 (154)	0.09 ± 0.02 (139)
II	0.26 ± 0.01 (278)	0.33 ± 0.01 (394)	0.14 ± 0.02 (324)
III	0.24 ± 0.01 (286)	0.24 ± 0.01 (419)	0.08 ± 0.02 (381)

[a] The SAOS-α2β1 cells were transfected with HA-tagged wild-type caveolin-3 or dominant negative caveolin for 48 h and then infected with EV1. Ten hours p.i., the cells were labeled with rabbit anti-EV1 and mouse anti-HA antibodies. The proportion of infected cells among the transfected ones was calculated using a confocal microscope. The experiment was carried out three times. The results are from three parallel samples. The number of cells used for the calculation is in parentheses.

[b] The reduction of infection due to Cav^{DGV} transfection was statistically significant ($P = 0.05$; Kruskal-Wallis one-way analysis of variance).

As a control we used another picornavirus, HPEV1, that we have previously shown to enter cells via the clathrin-dependent pathway (16). Expression of the dominant negative caveolin in A549 cells showed no significant reduction in the infection with HPEV1 (27% ± 0.1%, while the control was 28% ± 1%), suggesting that the dominant negative caveolin does not interfere with the clathrin-dependent pathway. Methyl β-cyclodextrin treatment, which affects cholesterol distribution and destroys caveolae, decreased the incidence of infection in cells exposed to virus from 63 to 9% (Table 2). Furthermore, methyl β-cyclodextrin decreased the amount of virus capsid proteins internalized to the perinuclear region (Table 2) and decreased the amount of cells showing perinuclear colocalization of EV1, caveolin-1, and α2β1 integrin, performed as pairwise labelings (Table 2).

DISCUSSION

Receptor-mediated entry and conformational changes of EV1. In agreement with the previous studies (6, 7, 42), EV1 infection in SAOS-α2β1 cells could be blocked by using antibodies against either α2 integrin subunit or β2 microglobulin. It is not currently clear whether β2 microglobulin acts as a coreceptor or whether its involvement in EV1 entry is indirect.

The receptor-mediated conformational alterations in the virion structure are considered to be an essential step in the internalization and genome release of picornaviruses. Whether the release of their RNA takes place in intracellular vesicles (as in the clathrin-mediated endocytosis route) or directly through the cellular plasma membrane is still unclear. The sucrose gradient centrifugation analysis showed a shift from the native 160S form to approximately 135S particles shortly after EV1 binding on the surface of SAOS-α2β1 cells, prior to the temperature shift needed for internalization of the virus. It is not clear, however, whether this conformational change is directly due to binding of the virus to α2 integrin, or whether virus binding to the receptor enhances interaction with some other membrane protein(s). Our unpublished results suggest that the so-called 135S particles of EV1 might differ from those of poliovirus 1 (V. Pietiäinen and T. Hyypiä, unpublished results). When the internalization of the virus proceeded at 37°C, the proportional amount of intracellular 80S empty capsids increased remarkably during the first 2 h of infection. Since the

TABLE 2. Effect of methyl β-cyclodextrin on internalization of EV1 and incidence of infection

Methyl β-cyclodextrin	Expt 1[a]: % of cells infected at 10 h p.i.	Expt 2[b]: % of cells with perinuclear accumulations containing:			Expt 3[c]: EV1 (mean fluorescence) inside cells after 2 h p.i.
		EV1 and α2β1 integrin	Caveolin-1 and EV1	Caveolin-1 and α2β1 integrin	
Not added	63 (246)[d]	70 (60)	73 (101)	74 (80)	100 (50)
Added	9 (411)[e]	3 (112)	6 (95)	5 (130)	2 ± 1 (47)[e]

[a] Infectivity 10 h p.i. was calculated after fluorescent labeling of EV1 capsid proteins. Bright cytoplasmic staining was regarded as an infected cell.
[b] The proportional number of cells showing colocalization of EV1, capsid proteins, α2β1 integrin, and caveolin-1 in the perinuclear area.
[c] Internalization of EV1 was calculated as the fluorescence intensity in the central 2-μm-thick section of cells from confocal images.
[d] Numbers of cells analyzed are shown in parentheses.
[e] Statistical significance was measured using Kruskal-Wallis one-way analysis of variance ($P < 0.001$).

location where viral RNA is released from the capsid is difficult to determine by the currently available methods, more structural data on the virus-receptor interactions will be needed to understand these phenomena in more detail.

EV1 is internalized through caveolae in vesicles containing α2β1 integrin and caveolin-1. For picornaviruses, contradictory data about the entry mechanisms have been reported. For example, polioviruses have been suggested to infect cells through directly forming pores in the cell membrane (40), by clathrin-coated endocytosis (46, 47), or by crossing a membrane barrier in the form of a 135S particle leading to the further uncoating in the cytoplasm (19). Recently, DeTulleo and Kirchhausen compared the entry mechanisms of human rhinovirus 14 (HRV14) and poliovirus 1 in HeLa cells and, based on studies with mutated dynamin, suggested that HRV14 utilizes a clathrin-mediated endocytosis pathway, whereas poliovirus 1 does not appear to use this route (9). However, since dynamin is also needed for pinching off caveola vesicles from the plasma membrane (12, 25), the mutant dynamin does not distinguish between different endocytic pathways. Schober et al. have shown recently that internalization of the major group HRVs, which use ICAM-1 as their cellular receptor, leads to rupture of endosomes followed by release of subviral particles into the cytoplasm (37). The members of the minor receptor group of HRVs recognize low-density lipoprotein receptor, internalize into endosomes, and release their genomes into the cytoplasm through a pore in the endosomal membranes (31). We studied previously the entry pathway of HPEV1 and showed by colocalization with markers of the early and late endosomes that HPEV1 uses the clathrin-dependent pathway (16). Here, we tested further HPEV1 infection in cells expressing dominant negative caveolin, and as expected, we found no inhibition of infection, confirming that HPEV1 does not rely on the caveola route.

Endocytosis via caveolae has been previously proposed for two viruses, SV40 and respiratory syncytial virus (2, 17, 45). Interestingly, it has also been reported that both α2 and β1 integrin subunits associate with caveolin-1 (43, 44), the main protein component of caveolae (35). A close connection between α2β1 integrin and caveolin-1 is also proposed by our finding that antibody cross-linking of α2β1 integrin causes copatching of caveolin-1 (Marjomäki et al., unpublished). Here, the internalization of EV1 via caveolae was supported by several facts. First, a clear colocalization of the virus with caveolin-1 was detected by both confocal and electron microscopy as well as after immunoisolation with anti-caveolin-1-coated beads in cells which are rich in caveola-like membrane domains. Second, the internalized structures containing EV1 and α2β1 integrin did not colocalize with markers of the clathrin-dependent endocytosis pathway. Third, the endocytosis of EV1 could be prevented by expression of dominant negative caveolin, the same expression construct which can block the endocytosis of SV40 (2).

According to recent data, in addition to endocytic caveolar transport vesicles, there is a pool of caveolin-1 that is associated with a heat shock protein-chaperone-cholesterol complex trafficking from ER to the plasma membrane (41). Since EV1 and α2β1 integrin are translocated from the plasma membrane to the perinuclear region, they are most probably associated with the caveolin-1-containing endocytic transport vesicles. Evaluation of the immunoisolated caveola structures showed that, in addition to EV1 capsid proteins, they contain α2β1 integrin and, based on infectivity titration, also infective virus. More precise knowledge of the localization and timing of RNA release from the capsid will help us to understand the mechanisms of caveola-mediated endocytosis in EV1 infection.

In the case of SV40, virus particles were found inside ER before the replication of the virus (17). Here, the EV1 capsid proteins were transported to perinuclear structures, rich in vesicles containing caveolin-1 and also α2β1 integrin, but negative for the used markers of ER. Thus, the internalization route of EV1 may be different from the one used by SV40.

The role of integrins in virus internalization. It is possible that the receptor largely determines the endocytosis route of the virus. Here, α2β1 integrin was not only required for endocytosis, but it was also internalized with the viral proteins. SV40 binds to major histocompatibility complex class I molecules and is translocated to the caveolin-enriched membrane domain (2, 3). However, major histocompatibility complex class I molecules are not internalized together with SV40 (3). Given the fact that integrins can bind to caveolin-1 (43), it is possible to hypothesize that EV1 takes advantage of this interaction to reach the caveolin-dependent endocytosis route. The process of integrin internalization after binding of soluble ligands is incompletely understood, and the same mechanisms that regulate integrin-mediated virus entry might be involved in the endocytosis of the natural ligands. For example, in endothelial cells α2β1 integrin mediates a pinocytic process leading to the formation of intracellular vacuoles that coalesce to form capillary lumens (8). Thus, mechanisms that regulate α2β1 integrin recycling may also have more general biological significance.

ACKNOWLEDGMENTS

We thank G. Banting, S. Fuller, H. Garoff, J. Gruenberg, M. McNiven, R. Parton, and H. Stenmark for the cDNAs and antibodies used in this study. The expert technical assistance of R. Hukkila, M. Lind, A. Mansikkaviita, S. Purola, M. Vainio, and R. Vassinen is gratefully acknowledged. T. Hovi is acknowledged for critical reading of the manuscript.

Financial support was provided by grants from the Academy of Finland, the Sigrid Jusélius Foundation, the University Central Hospitals of Turku and Helsinki, the Helsinki Graduate School in Biotechnology and Molecular Biology, and the Finnish Cancer Association.

REFERENCES

1. **Abraham, G., and R. J. Colonno.** 1984. Many rhinovirus serotypes share the same cellular receptor. J. Virol. **51:**340–345.
2. **Anderson, H. A., Y. Chen, and L. C. Norkin.** 1996. Bound simian virus 40 translocates to caveolin-enriched membrane domains, and its entry is inhibited by drugs that selectively disrupt caveolae. Mol. Biol. Cell **7:**1825–1834.
3. **Anderson, H. A., Y. Chen, and L. C. Norkin.** 1998. MHC class I molecules are enriched in caveolae but do not enter with simian virus 40. J. Gen. Virol. **79:**1469–1477.
4. **Banting, G., R. Maile, and E. P. Roquemore.** 1998. The steady state distribution of humTGN46 is not significantly altered in cells defective in clathrin-mediated endocytosis. J. Cell Sci. **111:**3451–3458.
5. **Barnstable, C. J., E. A. Jones, and M. J. Crumpton.** 1978. Isolation, structure and genetics of HLA-A, -B, -C and -DRw (Ia) antigens. Br. Med. Bull. **34:**241–246.
6. **Bergelson, J. M., M. P. Shepley, B. M. Chan, M. E. Hemler, and R. W. Finberg.** 1992. Identification of the integrin VLA-2 as a receptor for echovirus 1. Science **255:**1718–1720.
7. **Bergelson, J. M., N. St. John, S. Kawaguchi, M. Chan, H. Stubdal, J. Modlin, and R. W. Finberg.** 1993. Infection by echoviruses 1 and 8 depends on the alpha 2 subunit of human VLA-2. J. Virol. **67:**6847–6852.
8. **Davis, G. E., and C. W. Camarillo.** 1996. An alpha 2 beta 1 integrin-dependent pinocytic mechanism involving intracellular vacuole formation and coalescence regulates capillary lumen and tube formation in three-dimensional collagen matrix. Exp. Cell Res. **224:**39–51.
9. **DeTulleo, L., and T. Kirchhausen.** 1998. The clathrin endocytic pathway in viral infection. EMBO J. **17:**4585–4593.
10. **Grist, N. R., E. J. Bell, and F. Assaad.** 1978. Enteroviruses in human disease. Prog. Med. Virol. **24:**114–157.
11. **Gruenberg, J., and F. R. Maxfield.** 1995. Membrane transport in the endocytic pathway. Curr. Opin. Cell Biol. **7:**552–563.
12. **Henley, J. R., E. W. Krueger, B. J. Oswald, and M. A. McNiven.** 1998. Dynamin-mediated internalization of caveolae. J. Cell Biol. **141:**85–99.
13. **Huovila, A. P., A. M. Eder, and S. D. Fuller.** 1992. Hepatitis B surface antigen assembles in a post-ER, pre-Golgi compartment. J. Cell Biol. **118:** 1305–1320.
14. **Hynes, R. O.** 1992. Integrins: versatility, modulation, and signaling in cell adhesion. Cell **69:**11–25.
15. **Ivaska, J., H. Reunanen, J. Westermarck, L. Koivisto, V. M. Kähäri, and J. Heino.** 1999. Integrin $\alpha 2\beta 1$ mediates isoform-specific activation of p38 and upregulation of collagen gene transcription by a mechanism involving the $\alpha 2$ cytoplasmic tail. J. Cell Biol. **147:**401–416.
16. **Joki-Korpela, P., V. Marjomäki, C. Krogerus, J. Heino, and T. Hyypiä.** 2001. Entry of human parechovirus 1. J. Virol. **75:**1958–1967.
17. **Kartenbeck, J., H. Stukenbrok, and A. Helenius.** 1989. Endocytosis of simian virus 40 into the endoplasmic reticulum. J. Cell Biol. **109:**2721–2729.
18. **Kawaguchi, S., J. M. Bergelson, R. W. Finberg, and M. E. Hemler.** 1994. Integrin alpha 2 cytoplasmic domain deletion effects: loss of adhesive activity parallels ligand-independent recruitment into focal adhesions. Mol. Biol. Cell **5:**977–988.
19. **Kronenberger, P., R. Vrijsen, and A. Boeye.** 1992. Compartmentalization of subviral particles during poliovirus eclipse in HeLa cells. J. Gen. Virol. **73:**1739–1744.
20. **Kurzchalia, T. V., and R. G. Parton.** 1999. Membrane microdomains and caveolae. Curr. Opin. Cell Biol. **11:**424–431.
21. **Marjomäki, V. S., A. J. Huovila, M. A. Surkka, I. Jokinen, and A. Salminen.** 1990. Lysosomal trafficking in rat cardiac myocytes. J. Histochem. Cytochem. **38:**1155–1164.
22. **Mu, F. T., J. M. Callaghan, O. Steele-Mortimer, H. Stenmark, R. G. Parton, P. L. Campbell, J. McCluskey, J. P. Yeo, E. P. Tock, and B. H. Toh.** 1995. EEA1, an early endosome-associated protein. EEA1 is a conserved alpha-helical peripheral membrane protein flanked by cysteine "fingers" and contains a calmodulin-binding IQ motif. J. Biol. Chem. **270:**13503–13511.
23. **Mukherjee, S., R. N. Ghosh, and F. R. Maxfield.** 1997. Endocytosis. Physiol. Rev. **77:**759–803.
24. **Norkin, L. C.** 1999. Simian virus 40 infection via MHC class I molecules and caveolae. Immunol. Rev. **168:**13–22.
25. **Oh, P., D. P. McIntosh, and J. E. Schnitzer.** 1998. Dynamin at the neck of caveolae mediates their budding to form transport vesicles by GTP-driven fission from the plasma membrane of endothelium. J. Cell Biol. **141:**101–114.
26. **Oh, P., and J. E. Schnitzer.** 1999. Immunoisolation of caveolae with high affinity antibody binding to the oligomeric caveolin cage. J. Biol. Chem. **274:**23144–23154.
27. **Parton, R. G.** 1996. Caveolae and caveolins. Curr. Opin. Cell Biol. **8:**542–548.
28. **Parton, R. G., and M. Lindsay.** 1999. Exploitation of major histocompatibility complex class I molecules and caveolae by simian virus 40. Immunol. Rev. **168:**23–31.
29. **Pelkmans, L., J. Kartenbeck, and A. Helenius.** 2001. Caveolar endocytosis of simian virus 40 reveals a new two-step vesicular-transport pathway to the ER. Nat. Cell Biol. **3:**473–483.
30. **Pierschbacher, M. D., and E. Ruoslahti.** 1984. Variants of the cell recognition site of fibronectin that retain attachment-promoting activity. Proc. Natl. Acad. Sci. USA **81:**5985–5988.
31. **Prchla, E., C. Plank, E. Wagner, D. Blaas, and R. Fuchs.** 1995. Virus-mediated release of endosomal content in vitro: different behavior of adenovirus and rhinovirus serotype 2. J. Cell Biol. **131:**111–123.
32. **Roivainen, M., T. Hyypiä, L. Piirainen, N. Kalkkinen, G. Stanway, and T. Hovi.** 1991. RGD-dependent entry of coxsackievirus A9 into host cells and its bypass after cleavage of VP1 protein by intestinal proteases. J. Virol. **65:** 4735–4740.
33. **Roivainen, M., L. Piirainen, T. Hovi, I. Virtanen, T. Riikonen, J. Heino, and T. Hyypiä.** 1994. Entry of coxsackievirus A9 into host cells: specific interactions with alpha v beta 3 integrin, the vitronectin receptor. Virology **203:** 357–365.
34. **Rojo, M., R. Pepperkok, G. Emery, R. Kellner, E. Stang, R. G. Parton, and J. Gruenberg.** 1997. Involvement of the transmembrane protein p23 in biosynthetic protein transport. J. Cell Biol. **139:**1119–1135.
35. **Rothberg, K. G., J. E. Heuser, W. C. Donzell, Y. S. Ying, J. R. Glenney, and R. G. Anderson.** 1992. Caveolin, a protein component of caveolae membrane coats. Cell **68:**673–682.
36. **Roy, S., R. Luetterforst, A. Harding, A. Apolloni, M. Etheridge, E. Stang, B. Rolls, J. F. Hancock, and R. G. Parton.** 1999. Dominant-negative caveolin inhibits H-Ras function by disrupting cholesterol-rich plasma membrane domains. Nat. Cell Biol. **1:**98–105.
37. **Schober, D., P. Kronenberger, E. Prchla, D. Blaas, and R. Fuchs.** 1998. Major and minor receptor group human rhinoviruses penetrate from endosomes by different mechanisms. J. Virol. **72:**1354–1364.
38. **Stang, E., J. Kartenbeck, and R. G. Parton.** 1997. Major histocompatibility complex class I molecules mediate association of SV40 with caveolae. Mol. Biol. Cell **8:**47–57.
39. **Suomalainen, M., and H. Garoff.** 1994. Incorporation of homologous and heterologous proteins into the envelope of Moloney murine leukemia virus. J. Virol. **68:**4879–4889.
40. **Tosteson, M. T., and M. Chow.** 1997. Characterization of the ion channels formed by poliovirus in planar lipid membranes. J. Virol. **71:**507–511.
41. **Uittenbogaard, A., and E. J. Smart.** 2000. Palmitoylation of caveolin-1 is required for cholesterol binding, chaperone complex formation, and rapid transport of cholesterol to caveolae. J. Biol. Chem. **275:**25595–25599.
42. **Ward, T., R. M. Powell, P. A. Pipkin, D. J. Evans, P. D. Minor, and J. W. Almond.** 1998. Role for $\beta 2$-microglobulin in echovirus infection of rhabdomyosarcoma cells. J. Virol. **72:**5360–5365.
43. **Wary, K. K., A. Mariotti, C. Zurzolo, and F. G. Giancotti.** 1998. A requirement for caveolin-1 and associated kinase Fyn in integrin signaling and anchorage-dependent cell growth. Cell **94:**625–634.
44. **Wei, Y., M. Lukashev, D. I. Simon, S. C. Bodary, S. Rosenberg, M. V. Doyle, and H. A. Chapman.** 1996. Regulation of integrin function by the urokinase receptor. Science **273:**1551–1555.
45. **Werling, D., J. C. Hope, P. Chaplin, R. A. Collins, G. Taylor, and C. J. Howard.** 1999. Involvement of caveolae in the uptake of respiratory syncytial virus antigen by dendritic cells. J. Leukoc. Biol. **66:**50–58.
46. **Willingmann, P., H. Barnert, H. Zeichhardt, and K. O. Habermehl.** 1989. Recovery of structurally intact and infectious poliovirus type 1 from HeLa cells during receptor-mediated endocytosis. Virology **168:**417–420.
47. **Zeichhardt, H., K. Wetz, P. Willingmann, and K. O. Habermehl.** 1985. Entry of poliovirus type 1 and mouse Elberfeld (ME) virus into HEp-2 cells: receptor-mediated endocytosis and endosomal or lysosomal uncoating. J. Gen. Virol. **66:**483–492.
48. **Ziegler, T., M. Waris, M. Rautiainen, and P. Arstila.** 1988. Herpes simplex virus detection by macroscopic reading after overnight incubation and immunoperoxidase staining. J. Clin. Microbiol. **26:**2013–2017.